World Conference on
Timber Engineering
Oslo 2023

CROSS-LAMINATED TIMBER FLOORS WITH OPENINGS – SERVICEABILITY LIMIT STATE VERIFICATIONS

Martin Schenk[1], Anja Husel[2], Philipp Dietsch[3], Pablo González-Serna[4], José Manuel Cabrero[5], Stefan Winter[6]

ABSTRACT: This paper contributes information about the influence of openings in cross laminated timber (CLT) floors in serviceability limit state (SLS) design. SLS verifications according to the European structural design standard for timber structures - Eurocode 5 - comprise functionality, appearance and the user's comfort. The verifications are based on deformation and vibration criteria. The investigation presented describes the influence of openings on the basis of experimental and theoretical investigations. Rectangular centralized openings in CLT elements were tested. The experimental results were used for the calibration of the numerical models used for theoretical investigations. The numerical models were geometrically parameterized. Towards application for practice, modification factors were derived to enable determination of the respective deformation and first natural frequency.

KEYWORDS: mass timber, cross laminated timber, serviceability, openings in floors, deformation, vibration

1 INTRODUCTION

Structural design of openings in walls and floors is of crucial interest to enhance the competitiveness of cross-laminated timber (CLT) with other building materials [1]. Already for spans larger than 4 m – 5 m, serviceability limit state design (SLS) is decisive for the height of floor constructions in timber buildings [2]. Openings, e.g. for staircases or passages of technical building equipment (pipes, ventilation, etc.) locally reduce the mass and stiffness of floors and have therefor an influence on this important design situation. The verifications of serviceability limit states according to the European structural design standards [3], the Eurocodes, ensure (a) the functionality under typical conditions of use, (b) the appearance of the structure and (c) the comfort of intended users. According to the European design rules for timber structures [4] those verifications comprise criteria on deformations for (a-b) and on vibrations for (c). Research results on the performance of CLT floors with openings are available in e.g. [5, 6]. As presented in [7], simplified rules for the assessment and design of openings in CLT floors seem to vary significantly worldwide.

Striving towards a harmonization of rules, the aim of the present investigations is to contribute to existing studies on the influence of openings in CLT floors on SLS design. To achieve this, static load and vibration tests of 6 CLT elements by one single manufacturer without and with openings were carried out at the laboratories of the Technical University of Munich, Germany (MPA BAU), see Figure 1. Four-point bending tests were conducted to obtain the (i) stiffness, (ii) strength, (iii) deformations, and (iv) failure modes of the single span CLT elements. Vibration tests were conducted to derive the (v) natural frequencies of the system. The influence of openings was investigated for two sizes of openings, see Figure 2 and Figure 3. The test results, presented in Chapter 2 and in the companion paper [8], not only gave an insight into the structural behaviour of the system, but also provided data that has been used for the calibration of a numerical model, see Chapter 3, followed by a parametrized

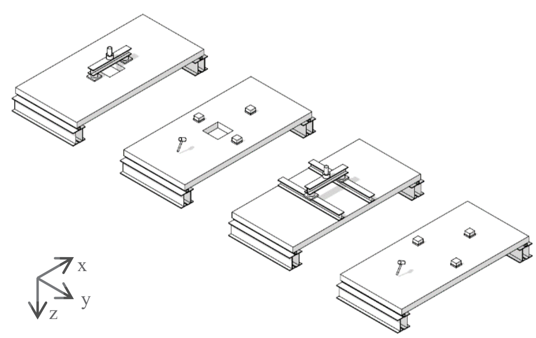

Figure 1: Deformation and vibration test set-up for a single span CLT floor with and without opening

[1] Martin Schenk, TUM Technical University of Munich, Germany, martin.schenk@tum.de
[2] Anja Husel, KIT Karlsruhe Institute of Technology, Germany, anja.husel@web.de
[3] Philipp Dietsch, KIT Karlsruhe Institute of Technology, Germany, dietsch@kit.edu
[4] Pablo González-Serna, UNAV University of Navarra, Spain, glezsernapablo@gmail.com
[5] José Manuel Cabrero, UNAV University of Navarra, Spain, jcabrero@unav.es
[6] Stefan Winter, TUM Technical University of Munich, Germany, winter@tum.de

https://doi.org/10.52202/069179-0351

numerical study on the influence of openings on deformations and frequencies in the system, see Chapter 4.

2 EXPERIMENTAL INVESTIGATIONS

A total of six non-edge-glued CLT specimens according to ETA-06/0138 [9] with an element height of 100 mm were tested in bending to determine the element stiffness and natural frequencies. The test set-up for bending corresponded to the test provisions of EN 16351 [10] in conjunction with EN 408 [11]. The lamination height of the five layers of the elements was 20 mm each with the outer layers oriented in span direction, see Table 1 and Figure 4. The strength class of the sorted laminations corresponded to C24 according to EN 338 [12]. The elements had a length of 2,50 m and width of 1,20 m. The span of the simple supported test set-up was 2,40 m. The ratio of plate thickness *t* to span *L* was 1/24.

Table 1: *Layer thickness and orientation relative to the x-axis of the element and total element thickness*

layer	1	2	3	4	5	Σ	unit
thickness	20	20	20	20	20	100	[mm]
orientation	0	90	0	90	0	–	[°]

The panels where tested in three series: (i) without opening, (ii) with an opening size of 300 mm x 300 mm and (iii) with an opening size of 600 mm x 300 mm, each in the centre of the elements, see Figure 2. Thus, the opening size corresponded to 12,5 % of the span and to 25 % of the panel width in case (ii) and to 50 % of the panel width in case (iii). In the test series with small opening (ii), the edge distance of the opening was 450 mm. In the test series with bigger opening (iii), the edge distance was 300 mm. Four panels (A2, A3, A4, A6) were tested in all opening stages while two panels (A1, A5) served as reference panels without openings. In this evaluation, the series with openings are presented. All CLT specimens were stored in standard climate until moisture balance with a temperature of around 20 °C and a relative humidity of about 65 % in the test laboratory. The mass of all panels and the moisture content of the CLT panels was determined according to EN 13183-2 [13], see Table 2. The elements had a mean density of 437,5 kg/m^3 (COV: 10,2) and an average moisture content of 11,3 m-% (COV: 0,083). Three different load configurations were tested: (a) two uniformly distributed linear loads over the full element width, (b) two concentrated point loads, both for deformation investigations and (c) an unloaded state for vibration investigations (self-weight only), see Figure 2. The loads *F* were applied with a displacement-controlled hydraulic actuator in the distance of 900 mm to the supports. The hydraulic cylinder was jointed to a self-contained steel frame, fixed to the ground. The point loads were applied via steel plates of 200 mm x 200 mm width, the linearly distributed loads via two respective spreader beams (HEB), which were linked with a steel coupler. To avoid compressive deformations perpendicular to the grain in the outermost layers, a hardwood lamella was placed as load distributing element onto the roller supports, see Figure 4. Via nine displacement transducers (w1-w9 in Figure 2), global and local deformations were recorded.

Table 2: *Average moisture content according to EN 13183-2 [13] and total element mass without opening*

specimen	A2	A3	A4	A6	unit
moisture	11,3	11,2	11,6	10,9	m-%
mass	132	132	130	131	[kg]

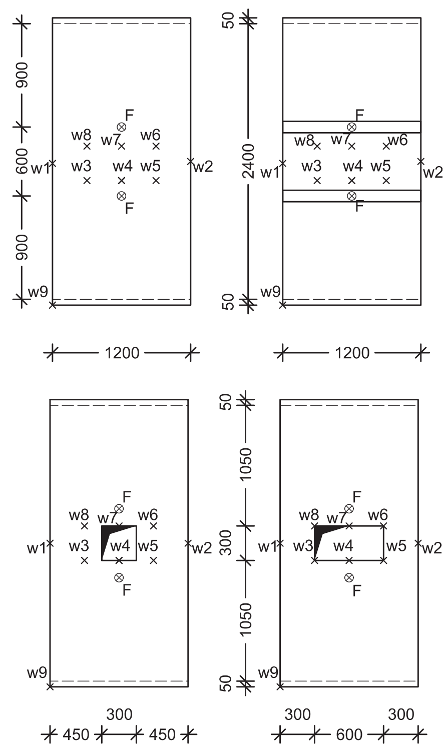

Figure 2: *CLT deformation tests: plan view with locations of the displacement transducers (w1-w9) and distributed load / concentrated load*

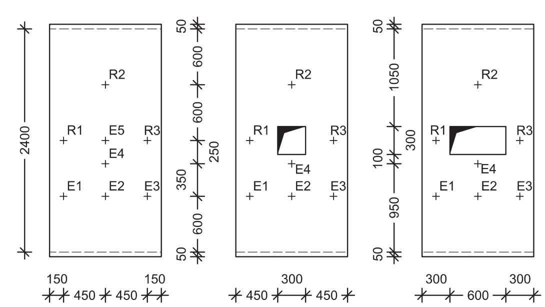

Figure 3: *CLT vibration tests: plan view of excitation points (E1-E5) and locations of the reception (R1-R3)*

https://doi.org/10.52202/069179-0351

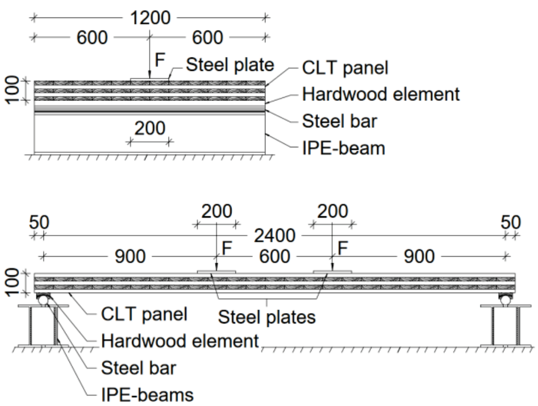

Figure 4: *CLT tests: side view in width (above) and length (below) direction*

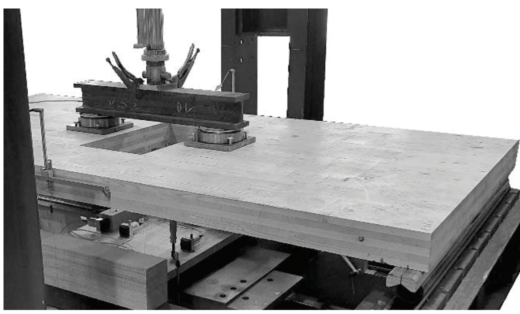

Figure 5*: View on the bending test set-up*

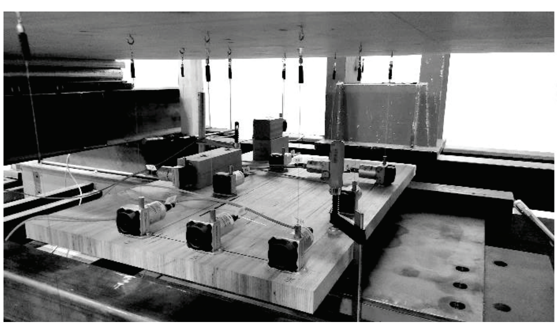

Figure 6: *View on displacement transducer arrangement*

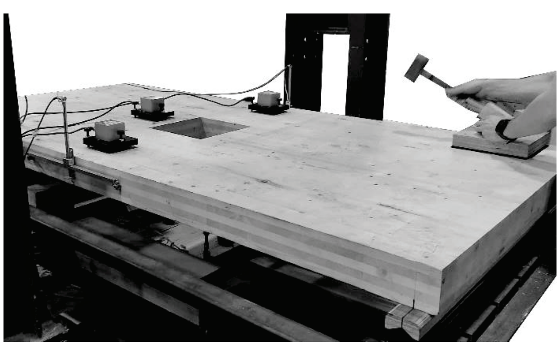

Figure 7: *View on the vibration test set-up*

Spherical bearings at the cylinder and at the concentrated loads ensured uniformly orthogonal load application, see Figure 5. Each concentrated load corresponded to the load $F/2$. An estimated failure load $F_{\mathrm{max,est}}$ was determined by numerical calculations according to [14]. In order to achieve deformations in the elastic range and also to reduce the risk of damage such as cracks or plastic deformations to the specimen, a conservative load limitation $F_{\mathrm{lim,est}}$ to 40 % of the estimated maximum load $F_{\mathrm{max,est}}$ was made for the non-destructive deformation tests. The non-destructive tests were stopped manually when the estimated limit load was reached. For, e.g. panel A2, the estimated limit load $F_{\mathrm{lim,est}}$ reached approximately 34 % of the destructively tested limit load $F_{\mathrm{max,test}}$, see Figure 8 and Figure 9. Figure 10 shows the evaluated moduli of elasticity in span direction x as average between the left panel edge (transducer w1) and the right panel edge (transducer w2) for all test series in load configuration (a) and (b). The specimens in this series were tested without opening. The in total smallest evaluated value of the modulus of elasticity was $E_{\mathrm{net,x,min}} = 12.468$ N/mm^2. The in total largest evaluated value of the modulus of elasticity was $E_{\mathrm{net,x,max}} = 14.558$ N/mm^2. The mean values were evaluated as $E_{\mathrm{net,x,mean}} = 13.596$ N/mm^2 in case (a) and $E_{\mathrm{net,x,mean}} = 13.243$ N/mm^2 in case (b), see Figure 10. The corresponding value according to the manufacturer was 12.000 N/mm². One reason for the relatively high tested values could be the inclusion of higher quality boards in

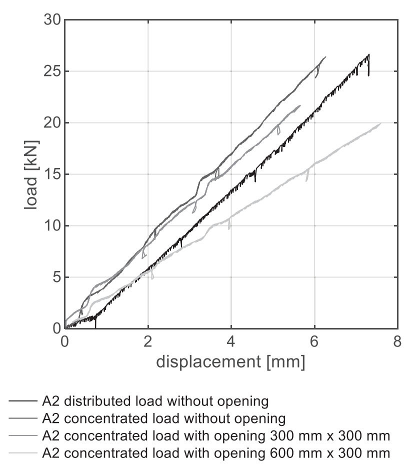

Figure 8: *Example of a load-displacement curve of specimen A2 at global w2 (non-destructive test until* $F_{lim,est} = 0,4 \cdot F_{max,est}$*)*

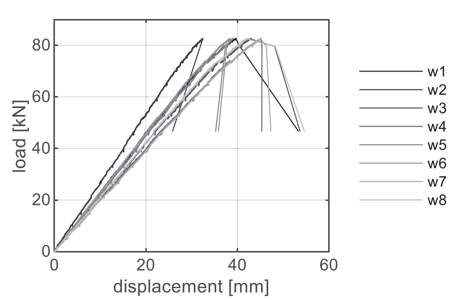

Figure 9: *Overview of load-displacement curves at all transducers of specimen A2 with concentrated load and opening 600 mm x 300 mm (destructive test) according to [15]*

https://doi.org/10.52202/069179-0351

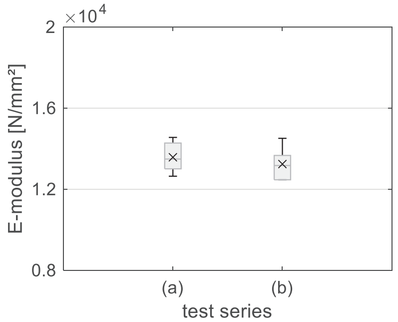

Figure 10: *(a) E-modulus tested according to [9] with uniformly distributed linear load without opening and (b) equivalent E-modulus tested with concentrated load without opening*

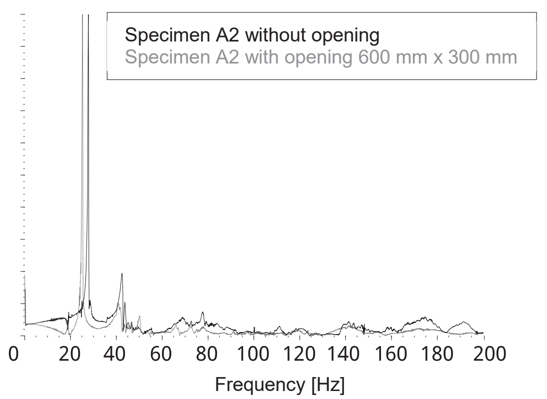

Figure 11: *Example of a vibration test of specimen A2 at locations E3 and R3*

Table 3: *Fundamental natural frequency of the CLT elements at locations E3 and R3: tested (A2 – A6) and simulated (FEA)*[*]

	frequencies [Hz]		
specimen	without opening	with opening 300 mm x 300 mm	with opening 600 mm x 300 mm
A2	27,6	26,6	25,2
A3	27,7	27,4	26,0
A4	26,5	26,1	24,7
A6	27,8	27,2	24,5
mean	27,4	26,8	25,1
FEA[*]	29,8	28,0	24,5

[*] see Chapter 3

the grading process. While the laminations have a stiffness more than 10 % higher than stated in declaration of performance, the resulting values for series (a) and (b) are at similar level. The averaged modulus of elasticity $E_{net,x,mean}$ in the case of testing according to [10] (a) is 2,6 % higher than the respective value in the case of concentrated loading (b). To obtain the dynamic characteristics of the elements, the CLT panels were excited at midspan, in the quarter points and at the opening edge by a falling impact hammer in all test stages, see Figure 7 and E1 – E5 in Figure 3. The response was read via accelerometers fixed to the panels in midspan and in the quarter of the span, see Figure 7 and R1 – R3 in Figure 3. The time history acceleration responses from the hammer impacts were converted into frequency domain using the Fast Fourier Transform algorithm, see Figure 11. Table 3 shows the first natural frequency of the elements with and without openings. In general, the first natural frequency of the CLT panels without openings was relatively similar in all elements. The mean fundamental frequency of the CLT panels without opening was 27,4 Hz. With opening, the scatter of the measured fundamental frequencies was a little wider, see Table 3. Due to an opening of 300 mm x 300 mm in the elements, the mean value for the natural frequency of the panels dropped by 2,2 % to 26,8 Hz. An extended opening width of 600 mm x 300 mm lead to a further decrease of the mean value of the fundamental frequency to 25,1 Hz and thus by 8,4 % compared to the condition without opening. For an in-depth view into the determination of values according to EN 384 [16], destructive test-results and further test- set ups, their execution and evaluation see the companion paper [8].

3 NUMERICAL INVESTIGATIONS

There are numerical or analytical methods for solving the plate differential equations, see e.g. [17 – 19], the latter usually being valid for very special cases only. In the present study, a linear elastic finite element (FE) analysis with the software SOFiSTiK 2020 (version 2020.13-1) [20] was used for numerical evaluations.

There are various ways of representing the material and load-bearing behaviour of cross laminated timber elements in finite element models. Figure 12 shows the considered models: (A) modelling of each individual lamination as 2D Timoshenko-beam element, (B) modelling as a multi-layered structure with shell elements and (C) modelling as an equivalent single layered shell element with adjusted material values. For the discussion of further structural models of CLT elements with openings, see [8]. For an overview of the advantages and disadvantages of the investigated model types (A) – (C), see [15].

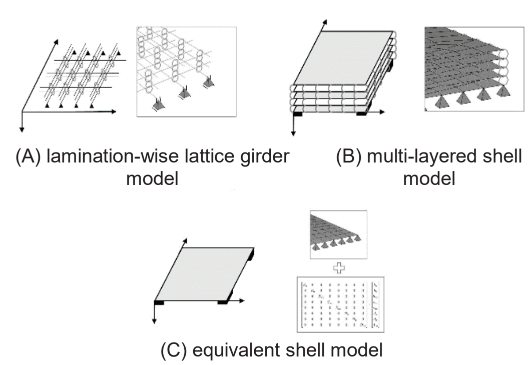

Figure 12: *Overview of considered FE models [13]*

https://doi.org/10.52202/069179-0351

The investigation on hand was carried out using 4-noded Bathe-Dvorkin shell elements, to avoid locking effects [20], with adapted stiffness properties (type C in Figure 12). Further information on locking effects can be found in [21] and [22]. A regular mesh size of the finite elements with a maximum width of 50 mm was chosen. For a convergence study on the mesh size, see [15]. In the applied models, the support conditions were fixed against translation in the *y*- and *z*-directions on one side of the span and against translations in *x*-, *y*- and *z*-directions on the other side. Both support conditions did not fix torsional deformations. A uniformly distributed load of 5 kN/m² was applied to the model for the evaluation of parametrized deformations.

Due to ratio of the investigated total panel thickness t to the span L, it might be assumed that deformations due to shear would not contribute considerably to the calculation results and might be neglected according to Kirchhoff's plate theory. According to Mestek [23], shear deformations of the cross-laminated timber panels may be neglected in the mechanical modelling for threshold ratios t/L = 1/20 …1/30. Additionally, Mestek [23] recommends to always consider shear deformation in serviceability limit state verifications. For the investigation on hand, shear deformations were considered throughout the models. The examined cross-laminated timber panels did not have edge bonding on the narrow edges of the laminations. Therefore, the Poisson's ratios were generally set to zero. For the same reason, the modulus of elasticity perpendicular to the grain in plane was set to zero as well. The adjustment of the torsional stiffness B_{xy} was made according to the declarations specified by the manufacturer [9]. For an in-deep view into the material properties of cross laminated timber, see e.g. Brandner et al. [24]. The applied stiffness values based on the test results are shown in Table 4. For a deeper insight into the evaluation of these stiffness values by calibration on the test results according to Chapter 2, see [15]. For the evaluation of the natural frequencies under dead load, the method according to Lanczos [25] was used. For an in-depth view into modelling of natural frequencies of CLT and respective model uncertainties, see e.g. Labonnote and Malo [26]. The numerical model was parameterized in the geometries span of the element L_x = 3.000…7.000 mm, width of the opening l_y = 0,10…0,80 · L_y and length of the opening l_x = 1.000…1.500 mm according to Figure 13.

Table 4: *Material parameters for the model evaluated in [15]*

B_x [kNm/m]	B_y [kNm/m]	B_{xy} [kNm/m]	S_{xz} [kN/m]	S_{yz} [kN/m]
792	208	33,8	7.980	4.420

B_x; B_y = bending stiffness
B_{xy} = torsional stiffness
S_{xz}; S_{yz} = shear stiffness

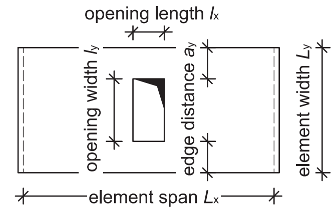

Figure 13: *Definition of geometries according to [15]*

4 RESULTS

The results of the calibrated and parameterized FE analysis were internal forces and deformations, each in the respective element nodes, as well as natural frequencies. The post-processing of the data was carried out with SOFiSTiK, Microsoft Excel and a Python script. Under the two concentrated loads, the CLT elements deformed in both the longitudinal and transversal direction, see Figure 14. The deformed shape of the CLT panels with and without openings was similar under the uniformly distributed load of 5 kN/m². The maximum deflection occurred usually in the area of transducer w4 respectively w7, see Figure 2. The first eigenmode, each with and without opening, reflected an expected semi-sinusoidal shape, see Figure 15.

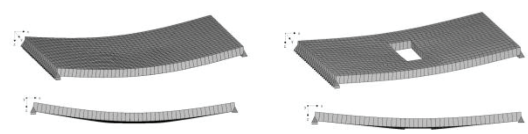

(A) without opening (B) with opening 600 mm x 300 mm

Figure 14: *Deformed shape of the CLT element with visualized element height [15]*

(A) without opening (B) with opening 600 mm x 300 mm

Figure 15: *Semi-sinusoidal eigenmode of the CLT element*

Figure 16 shows the non-normally distributed scatter of the maximum deformation expressed as increase factor k_w, normalized on the deformation without opening for centralized rectangular openings with a fixed opening length of l_x = 1.000 mm, see Figure 16 (A), and length of l_x = 1.500 mm, see Figure 16 (B), respectively, and a span parametrized between L_x = 3.000…7.000 mm according to equation (1). Table 5 lists the respective mean values.

$$k_X = \frac{X_2}{X_1} \quad (1)$$

with

$X = w$ for the deformation (2)

$X = f_1$ for the first natural frequency (3)

where

k_X = influence factor of the opening on an effect of action named X;

X_1 = value of the effect of action without opening;

X_2 = value of the effect of action with opening.

It was noted that the relative influence of the opening width l_y on the deformation increases exponentially with the increase of the same in the investigated set-up. As expected with a uniaxial load-bearing system, increasing the opening length l_x in span direction has positive effect on the deformations in case of large opening widths, see Figure 16. From the data obtained, it also appears that the influence of the opening width l_y increases as the span increases. The observations on the deformation can be transferred to the eigenvalues, see Figure 17. Here, too, the influence increases more with increasing opening width compared to increasing opening length. In addition to the stiffness, the influence of the reduced self-weight due to the opening on the natural frequency should not be neglected.

Table 5: *Mean values of influence factor k_w according to [15] and k_{f1} for a span in the range of L_x = 3.000…7.000 mm and for an opening length l_x = 1.000 mm*

l_y/L_y	0,10	0,25	0,50	0,67	0,80
k_w	1,02	1,15	1,54	2,12	3,04
k_{f1}	0,99	0,94	0,83	0,72	0,60

l_y = opening width
L_y = element width

5 CONCLUSIONS AND OUTLOOK

Eurocode 5 provides SLS design verifications for functionality, appearance and the user's comfort in form of deformation and vibration criteria [4]. According to the current draft of the second generation of Eurocode 5 [27], deformations have to be verified using the characteristic, frequent, or quasi-permanent combination of actions given in Eurocode 0 [28]. Based on the investigations of e.g. [29 – 31], vibration verification according to prEN 1995-1-1 [27] comprises frequency criteria, stiffness criteria, velocity and acceleration criteria which are adapted to human perception. The investigations presented showed that openings in CLT floors have a decisive influence on the deformations and the natural frequencies and hence influence the respective verifications in SLS design. Simplified design rules for the verification of deformations of CLT floors with openings do not yet exist in the European design standard.

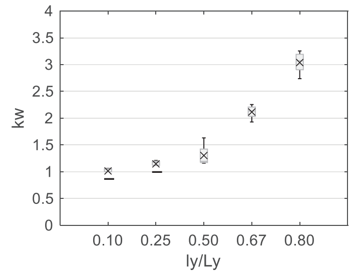

(A) l_x = 1.000 mm

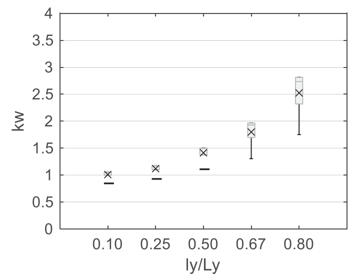

(B) l_x = 1.500 mm

Figure 16: *Non-normally distributed scatter of the increase factor k_w for a span in the range of L_x = 3.000…7.000 mm under uniformly distributed load of 5 kN/m² according to [15]*

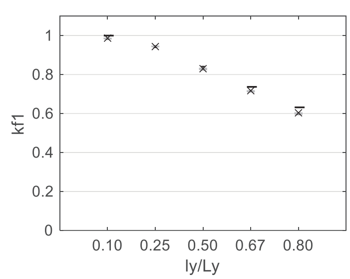

(A) l_x = 1.000 mm

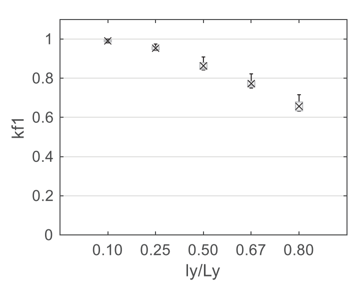

(B) l_x = 1.500 mm

Figure 17: *Non-normally distributed scatter of the increase factor k_{f1} for a span in the range of L_x = 3.000…7.000 mm under self-weight*

https://doi.org/10.52202/069179-0351

According to prEN 1995-1-1 [27], under certain boundaries, openings in floors may be generally neglected in the vibration verification provided that the plan area of the opening area and that no individual opening dimension is greater than 40 % of the respective floor dimension.

Further introduction of simplified rules for SLS design of CLT floors with openings would not only strengthen the competitiveness of timber structures but could also support the resource-efficient use of the material in general. Subsequently, with further harmonisation of its structural design, application of CLT will become more and more user-friendly and attractive globally [32].

ACKNOWLEDGEMENT

Project InnoCrossLam was supported under the umbrella of ERA-NET Cofund ForestValue by MIZŠ, INNOVA, FORMAS, STEM, BMLFUW, FNR and MINECO-AEI and has received funding from the European Union's Horizon 2020 research and innovation programme under grant agreement N° 773324.

The financial support provided by Fachagentur Nachwachsende Rohstoffe e. V. (FNR) of the German Federal Ministry of Food and Agriculture (BMEL) and the Spanish Ministerio de Ciencia, Innovación y Universidades – Agencia Estatal de Investigación under contract PCI2019-103591 AEI is gratefully acknowledged.

Special thanks go to KLH Massivholz GmbH and the colleagues from UNAV, KIT and TUM for excellence collaboration.

REFERENCES

[1] Schenk M., González-Serna P., J. M. Cabrero: Future research on cross laminated timber (CLT) for multi-storey buildings – a questionnaire among engineers active in practice. In: Proceedings WCTE 2020, Chile, 2020/21.

[2] Moosbrugger Th., Bogensperger Th., Krenn H.; Bemessungsdiagramme für den biegebeanspruchten Stab im Holzbau – Teil 2: Deckentragwerke mit inhomogenen Stabquerschnitt. Bautechnik 92, 2015.

[3] EN 1990:2010 Basis of structural design; EN 1990:2002 + A1:2005 + AC:2010. Comité Européen de Normalisation (CEN), Belgium, 2010.

[4] EN 1995-1-1:2014 Eurocode 5: Design of timber structures – Part 1-1: General – Common rules and rules for buildings; EN 1995-1-1:2004 + AC:2006 + A1:2008 + A2:2014. Comité Européen de Normalisation (CEN), Belgium, 2014.

[5] Popovski M., Chen Z.; Structural behaviour of point-supported CLT floor systems. In: Proceedings WCTE 2016, Austria, 2016.

[6] Kozaric L., Bursac S., Vojnic Purcar M., Besevic M., Tekic Z.: Finite Element Analysis of Dynamic Characteristics and Bending Stiffness for Cross Lamianted Timber Floor Panels with and without Openings. Drvna Industrija, 2021.

[7] Arnold M., Schenk M., Kainz N., Dietsch P., Cabrero J. M.; Maderebner R.; Winter S.: Schlussbericht zum Europäischen Forschungsvorhaben InnoCrossLam – Innovative Lösungen für das zukünftige Bauen mit Brettsperrholz - Arbeitspakete 5 und 6 (Deutschland). Research report, Germany 2022.

[8] González-Serna P., Yurrita M., J. M. Cabrero: Experimental analysis of the influence of openings in cross-laminated timber plates loaded out of plane. In: Proceedings WCTE 2023, Norway, 2023.

[9] ETA-06/0138 based on EAD 130005-00-0304 – Solid wood slab element to be used as a structural element in buildings. Österreichisches Institut für Bautechnik (OIB), Austria, 2021.

[10] EN 16351:2021 Timber structures – Cross laminated timber – Requirements. Comité Européen de Normalisation (CEN), Belgium, 2021.

[11] EN 408:2012 Timber structures – Structural timber and glued laminated timber – Determination of some physical and mechanical properties; EN 408:2010+A1:2012. Comité Européen de Normalisation (CEN), Belgium, 2012.

[12] EN 338:2016 Structural timber – Strength classes. Comité Européen de Normalisation (CEN), Belgium, 2016.

[13] EN 13183-2:2002 Moisture content of a piece of sawn timber – Part 2: Estimation by electrical resistance method. Comité Européen de Normalisation (CEN), Belgium, 2002.

[14] González-Serna P. (unpublished): Proposal for testing CLT floor plates with openings. Internal paper, Spain, 2021.

[15] Husel A.: Preliminary studies on openings in cross laminated timber plates. Master thesis, Karlsruhe Institute of Technology, Germany, 2022.

[16] EN 384:2018 Structural timber – Determination of characteristic values of mechanical properties and density; EN 338:2016+A1:2018. Comité Européen de Normalisation (CEN), Belgium, 2018.

[17] Timoshenko T., Woinowsky-Krieger S.: Theory of plates and shells. American Society of Civil Engineers, United States of Amerika, 1959.

[18] Reddy J. N.: Mechanics of Laminated Composite Plates and Shells - Theory and Analysis, CRC Press, United States of Amerika, 1997.

[19] Bogensperger T., Silly G., Schickhofer G.: Comparison of Methods of Approximate Verification Procedures for Cross Laminated Timber. Research Report, Graz University of Technology, Austria, 2012.

[20] SOFiSTiK AG (ed): SOFiSTiK - Manual. Germany, 2020.

[21] Bathe K.-J., Dvorkin, E. N.: A continuum mechanics based four-node shell element for general non-linear analysis. Massachusetts Institute of Technology Cambridge, United States of Amerika, 1983.

[22] Koschnick F.: Geometrische Locking-Effekte bei Finiten Elementen und ein allgemeines Konzept zu ihrer Vermeidung. Dissertation, Technical University of Munich, Germany, 2004.

[23] Mestek P: Punktgestützte Flächentragwerke aus Brettsperrholz (BSP) – Schubbemessung unter

Berücksichtigung von Schubverstärkungen. Dissertation, Technical University of Munich, Germany, 2011.
[24] Brandner R., Flatscher G., Ringhofer A., Schickhofer G., Thiel A.: Cross laminated timber (CLT): overview and development. European Journal of Wood and Wood Products, Germany, 2016.
[25] Lanczos C.: An Iteration Method for the Solution of the Eigenvalue Problem of Linear Differential and Integral Operators. Journal of Research of the National Bureau of Standards, United States of Amerika, 1950.
[26] Labonnote N., Malo K. A.: Vibration properties of cross laminated timber floors. Proceedings ICSA 2010, Portugal, 2010.
[27] prEN 1995-1-1:2023 Eurocode 5: Design of timber structures – Part 1-1: General rules and rules for buildings. Comité Européen de Normalisation (CEN), Belgium, 2023.
[28] EN 1990:2023 Basis of structural design. Comité Européen de Normalisation (CEN), Belgium, 2023.
[29] Ohlsson S.: Floor Vibrations and Human Discomfort. Dissertation, Chalmers University of Technology, Sweden, 1982.
[30] Willford M. R., Young P.: A Design Guide for Footfall induced Vibration of Structures – A tool for designers to engineer the footfall vibration characteristics of buildings or bridges. The Concrete Society, United Kingdom, 2006.
[31] Hamm P., Marcroft J., Toratti T.: Vibrations of floors – Comparison of measured data and suggested design. INTER 53 - 20 – 1, International Network on Timber Engineering Research, Germany, 2020.
[32] Azinović A., et al.: InnoCrossLam – adding knowledge towards increased use of cross laminated timber (CLT). In: Proceedings WCTE 2023, Norway, 2023.

https://doi.org/10.52202/069179-0351